

Comparative Proteomics Analysis of the Postmitochondrial Supernatant Fraction of Human Lens-Free Whole Eye and Liver[§]

Ankit Balhara¹, Abdul Basit¹, Upendra A. Argikar, Jennifer L. Dumouchel, Saranjit Singh, and Bhagwat Prasad

Department of Pharmaceutical Analysis, National Institute of Pharmaceutical Education and Research (NIPER), S.A.S. Nagar, Punjab, India (An.B., S.S.); Department of Pharmaceutical Sciences, Washington State University, Spokane, Washington (Ab.B., B.P.); Biotransformation Group, Novartis Institutes for BioMedical Research, Cambridge, Massachusetts (U.A.A.); and Department of Molecular Pharmacology and Physiology, Brown University, Providence, Rhode Island (J.L.D.)

Received October 25, 2020; accepted April 8, 2021

ABSTRACT

The increasing incidence of ocular diseases has accelerated research into therapeutic interventions needed for the eye. Ocular enzymes play important roles in the metabolism of drugs and endobiotics. Various ocular drugs are designed as prodrugs that are activated by ocular enzymes. Moreover, ocular enzymes have been implicated in the bioactivation of drugs to their toxic metabolites. The key purpose of this study was to compare global proteomes of the pooled samples of the eye ($n = 11$) and the liver ($n = 50$) with a detailed analysis of the abundance of enzymes involved in the metabolism of xenobiotics and endobiotics. We used the postmitochondrial supernatant fraction (S9 fraction) of the lens-free whole eye homogenate as a model to allow accurate comparison with the liver S9 fraction. A total of 269 proteins (including 23 metabolic enzymes) were detected exclusively in the pooled eye S9 against 648 proteins in the liver S9 (including 174 metabolic enzymes), whereas 424 proteins (including 94 metabolic enzymes) were detected in

both the organs. The major hepatic cytochrome P450 and UDP-glucuronosyltransferases enzymes were not detected, but aldehyde dehydrogenases and glutathione transferases were the predominant proteins in the eye. The comparative qualitative and quantitative proteomics data in the eye versus liver is expected to help in explaining differential metabolic and physiologic activities in the eye.

SIGNIFICANCE STATEMENT

Information on the enzymes involved in xenobiotic and endobiotic metabolism in the human eye in relation to the liver is scarcely available. The study employed global proteomic analysis to compare the proteomes of the lens-free whole eye and the liver with a detailed analysis of the enzymes involved in xenobiotic and endobiotic metabolism. These data will help in better understanding of the ocular metabolism and activation of drugs and endobiotics.

Introduction

The liver is a major organ responsible for the biotransformation of xenobiotics and endobiotics due to the abundant hepatic expression of metabolizing enzymes. Although significant information on the metabolic capacity of organs such as liver, intestine, kidney, and lung is well documented (Nakamura et al., 2016; Drozdik et al., 2018; Couto et al., 2019; Oesch et al., 2019; Basit et al., 2020; Couto et al., 2020), the data on the ability of the eye to metabolize drugs and endobiotics is sparse (Al-Ghananeem and Crooks, 2007; Nakano et al., 2014; Argikar et al., 2017a). Although the eye serves as the site of first-pass metabolism for

the drugs that are administered directly to the eye via topical or local routes (such as subconjunctival, intravitreal, retrobulbar, and intracameral), some systemically administered drugs can also be metabolized in the eye (Thrimawithana et al., 2011; Gokulgandhi et al., 2012; Argikar et al., 2017b; Dumouchel et al., 2018). Analogous to the liver, drugs delivered into the eye are metabolized, activated, and cleared by the drug-metabolizing enzymes (DMEs) present therein (Argikar et al., 2017b). For example, latanoprostene bunod is hydrolyzed into two active components, latanoprost acid metabolite and nitric oxide in the eye (Garcia et al., 2016). Topical β -blockers such as levobunolol, betaxolol, caretolol, timolol, and metipranolol also form their active metabolites in the eye (Bushee et al., 2015; Argikar et al., 2016, 2017b). On the other hand, ketoconazole was observed to get bioactivated into a toxic iminium intermediate in the in vitro studies with eye S9 fraction (Cirello et al., 2017). Similar to the drugs, metabolism of endobiotics within the eye is a critical process for the normal eye function. For example, ocular enzymes play an important role in vitamin A and eicosanoid homeostasis in the eye (Stoltz et al., 1994; Connors et al., 1995; Duester 2001; Gallego et al., 2006; Kam et al., 2012).

This work was supported by funding from the Department of Pharmaceutical Sciences, Washington State University, Spokane, WA; Department of Pharmaceuticals, University of Washington, Seattle, WA; Novartis Institutes for BioMedical Research, Cambridge, MA; and National Institute of Pharmaceutical Education and Research (NIPER), S.A.S. Nagar, Punjab, India.

¹An.B. and Ab.B. contributed equally.

<https://doi.org/10.1124/dmd.120.000297>.

[§] This article has supplemental material available at dmd.aspetjournals.org.

ABBREVIATIONS: ADH, alcohol dehydrogenase; AKR, aldo-keto reductase; ALDH, aldehyde dehydrogenase; CAH, carbonic anhydrase; CES, carboxylesterase; CES1P1, carboxylesterase 4; COX, cytochrome c oxidase; DDA, data-dependent acquisition; DME, drug-metabolizing enzyme; EPHX, epoxide hydrolase; GST, glutathione S-transferase; HSD17B, 17- β -hydroxysteroid; LFQ, label-free quantification; MS, mass spectrometry; MS/MS, Tandem mass spectrometry; NAT, *N*-acetyl transferase; PCA, principal component analysis; RDH, retinol dehydrogenase; S9 fraction, postmitochondrial supernatant fraction; SULT, sulfotransferase; UGT, UDP-glucuronosyltransferase.

The eye has an extremely complex anatomy and its subcompartments have a wide range of physiologic functions. In vitro models derived from tissue sections or subcompartments do not allow for the study of drug or endobiotic metabolic activity due to reasons such as overdilution of protein content, high degree of nonspecific binding, and low abundance of metabolites in the homogenate, or artifactually limiting sequential metabolism (Argikar et al., 2017b; Dumouchel et al., 2018). Although individual ocular tissues from preclinical animal models are used in the pharma industry for the study of drug metabolism, these models are expensive and require sophisticated technical laboratory skills. Among the existing models, the lens-free whole eye postmitochondrial supernatant fraction (S9 fraction) has been used to a greater extent by the pharmaceutical industry for metabolism studies during early drug discovery stage (Dumouchel et al., 2018). Ocular S9 fraction is the supernatant collected after removing nuclei and mitochondria from the lens-free whole eye homogenate at $12,000 \times g$. It is a mixture of microsomes (representing endoplasmic reticulum) and cytosol that are enriched with metabolizing enzymes and can be customized with the cofactors for study of the metabolic function in vitro. Ocular S9 fraction has been applied recently to investigate metabolism of the drugs used for treating ocular ailments, e.g., levobunolol (Argikar et al., 2016), betaxolol (Bushee et al., 2015), ketoconazole (Cirello et al., 2017), and timolol (Dumouchel et al., 2017).

Although the evidence of the application of the eye S9 model is emerging in drug development, no report of a comprehensive proteomics investigation exists for the pooled ocular S9 fraction. Therefore, the focus of the present study was to explore human ocular S9 proteome and compare it with the human liver S9 proteome. To allow direct comparison between the organs, pooled S9 fraction from the eye ($n = 11$) and the liver ($n = 50$) were used, and a parallel investigation was carried out under identical conditions using aligned methodology. The pooled samples were used to generate information on an average virtual human population. In that respect, this study provides novel hypothesis-generating data, which is anticipated to be helpful in subsequent targeted proteomics, genomics, and functional studies to investigate efficacy and ocular toxicity of ophthalmic drugs and eye physiology.

Materials and Methods

Materials. Ammonium bicarbonate (98% purity), dithiothreitol, iodoacetamide, and Pierce trypsin protease (MS -grade) were purchased from Thermo Fisher Scientific (Rockford, IL). Sodium deoxycholate (98% purity) was obtained from MP Biomedicals (Santa Ana, CA). Chloroform, ethyl ether, Optima MS-grade acetonitrile, methanol, and formic acid were purchased from Fisher Scientific (Fair Lawn, NJ).

Ocular and Liver Tissue Procurement and Preparation of S9 Fractions. Pooled ocular S9 and pooled liver S9 fractions were procured from Sekisui XenoTech, LLC (Kansas City, KS). The eye tissue donors ($n = 11$) were males and females of Caucasian origin between 51 and 88 years. The liver tissue donors ($n = 50$) were males and females of Caucasian, African American, and Hispanic origin between 25 and 78 years. The pooled samples excluded donors with ocular and/or hepatic disorders. The S9 fractions were prepared by commonly accepted procedures for the preparation of subcellular fractions from organs subsequent to differential centrifugation (Levin et al., 1972; Argikar and Remmel, 2009a,b). In general, the tissues were thawed and homogenized in a 50 mM Tris-HCl buffer, pH 7.4, containing 150 mM potassium chloride and 2 mM EDTA. For eyes, the lenses were removed prior to homogenization. The remaining ocular tissues and fluids, including cornea, choroid, sclera, retina, aqueous humor, vitreous humor, iris, and ciliary body were present in the homogenate (Bushee et al., 2015; Argikar et al., 2016). The buffer volume in milliliters was approximately $3 \times$ the weight of the tissues in gram. The homogenate was centrifuged at $12,000 \times g$ for 20 minutes at 4°C . The supernatant from this spin was separated and stored at -80°C as S9 fraction until further use. The supernatant was free of mitochondria, nuclei, and other cell debris.

Protein Denaturation, Reduction, Alkylation, Enrichment, and Trypsin Digestion. Samples of pooled S9 fractions were trypsin-digested as described previously (Boberg et al., 2017; Bhatt et al., 2019). In brief, the process undertaken included denaturation and reduction of proteins in S9 fraction (2 mg/ml, 80 μl) with 10 μl dithiothreitol (250 mM) at 95°C . The sample was then cooled to room temperature and alkylated with 20 μl iodoacetamide (500 mM) in dark. The treated protein was subsequently precipitated with ice-cold methanol-chloroform (500 μl :100 μl). Subsequently, water (400 μl) was added to each sample to remove salts and polar impurities. The desalted samples were vortexed

and centrifuged at $16,000 \times g$ (4°C) for 5 minutes to result in a protein pellet, which was recovered by carefully removing and discarding the upper organic and lower aqueous layers. The pellet was then washed with ice-cold methanol (500 μl) and dried for 30 minutes at room temperature. It was resuspended in ammonium bicarbonate buffer (50 mM, 60 μl) and digested by trypsin (protein:trypsin ratio, approximately 50:1, 20 μl) at 37°C for 16 hours. The reaction was quenched by addition of 40% acetonitrile containing 0.5% formic acid and diluted with 0.1% formic acid to bring protein concentration to 1 $\mu\text{g}/\mu\text{l}$. The sample was vortex mixed and centrifuged at $4000 \times g$ for 5 minutes. The supernatant was collected in a liquid chromatography mass spectrometry (LC-MS) vial for further analyses.

Data-Dependent Acquisition. The untargeted proteomics analysis was conducted on a Q Exactive HF coupled with Easy Spray 1200 series nanoLC (Thermo Fisher Scientific, Waltham, MA). One μl of the sample ($\sim 1 \mu\text{g}/\mu\text{l}$ protein) was loaded onto a C18 trap column (Acclaim PepMap, 100 $\mu\text{m} \times 2 \text{ cm}$, 5 μm) at a flow rate of 5 $\mu\text{l}/\text{min}$, and sample loading was done with 0.1% formic acid in water. After loading and desalting for 10 minutes with 0.1% formic acid, the trap was brought in-line with an analytical column (Thermo Scientific PepMap RSLC C18, 50 $\mu\text{m} \times 15 \text{ cm}$, 2 μm). The mobile phase flow rate was 0.3 $\mu\text{l}/\text{min}$. Peptides were detected in data-dependent acquisition (DDA) method in full scan positive mode. The top 10 most intense ions from the parent ion scan (MS1 scan) were selected for the collision-induced dissociation. The charge state of the peptides was fixed between +2 to +6. Survey scans of peptide precursors were performed in the Orbitrap mass analyzer from 375 to 1500 m/z at 120,000 resolution (at 200 m/z) with a 3×10^6 ion count target and a maximum injection time of 100 millisecond. The instrument was set to run in top speed mode with 3 second cycles for the survey and the MS/MS scans. The MS/MS resolution was set to 15,000 with automatic gain control (AGC) target of 1×10^5 and maximum fill time of 100 millisecond with isolation window of 1.6 m/z . Normalized collision energy was 27. The samples were acquired in triplicate to minimize the technical variability.

Data Analysis. All six DDA data files of eye and liver S9 fractions were analyzed using MaxQuant software (version 1.6.8.0, Max Planck Institute of Biochemistry, Germany) with default settings (Tyanova et al., 2016; Beer et al., 2017). The protocol followed for the data analyses is shown in Fig. 1. The complete human proteome FASTA file was downloaded from Uniprot (<https://www.uniprot.org/>) in November, 2019. The complete proteome FASTA was manually curated to allow deeper analysis of endo- or xenobiotic metabolizing enzymes by using keywords such as “hydrolase,” “dehydrogenase,” “transferase,” “esterase,” “epoxidase,” “reductase,” “isomerase,” and “transporter,” by following the approaches reported elsewhere (Resing et al., 2004; Yen et al., 2006; Kumar et al., 2017). A total of 1187 protein entries were present in the curated FASTA file, which included cytochrome P450s, UDP-glucuronosyltransferases (UGTs), sulfotransferases (SULTs), *N*-acetyl transferases (NATs), glutathione transferases (GSTs), oxidases, aldo-keto reductases (AKRs), dehydrogenases, paraoxonases, mitochondrial amidoxime-reducing component, carboxylesterase (CES), coagulation factors, isomerases, and drug transporters. The complete human proteome FASTA file as well as the shortlisted files representing metabolic enzymes were used as the reference sequences in the Andromeda data base search tool of the MaxQuant software package. The primary parameters used during the search included: 1) digestion: specific digestion with trypsin/P; 2) peptide lengths: between 7 and 25 residues; 3) missed cleavage sites allowed: 2; 4) fixed modification: carbamidomethylation; 5) variable modifications: acetylation (protein N-term) and oxidation (M); 6) modifications per peptide allowed: 5; 7) mass tolerance for first peptide tolerance and main peptide tolerance: 20 ppm and 5 ppm, respectively; 8) minimum peptides: 2; 9) minimum razor + unique peptides: 2; 10) minimum unique peptides: 2; and 11) false discovery rate: 0.01 for both peptide and protein identification.

Relative Abundance of Proteins Common between Eye and Liver S9 Fractions. The proteins were quantified using a generic label-free quantification (LFQ) method (MaxLFQ) in MaxQuant software (Cox et al., 2014). The resulting MaxLFQ intensities of proteins present in both the eye and the liver S9 fractions were compared to get the relative abundance values. The list of identified proteins by MaxQuant were further processed using Perseus software (1.6.8.0) (Tyanova and Cox, 2018) to filter out: 1) the contaminants, 2) proteins identified by the reverse sequence, and 3) ambiguous identifications, i.e., proteins identified in only one replicate out of the three. The final list of proteins was subjected to principal component analysis (PCA) to identify the group-dependent clustering of the replicates and to reveal whether the eye proteome was significantly different from the liver proteome. Further, volcano plots were created to highlight the significantly different proteins between the eye and the liver S9 samples. To interpret the cellular context and biologic pathways associated with the protein identified in the eye S9 fraction, network association was performed using search tool for the retrieval of interacting genes/proteins (STRING) that provides knowledge on functional protein-protein interaction. Finally, the proteins detected in both the eye and the liver S9 samples were compared based on the ratios of the average LFQ intensities, as described by the following equation:

$$\text{Relative abundance of protein in eye versus liver} = \frac{\text{Average LFQ intensity in pooled eye sample}}{\text{Average LFQ intensity in pooled liver sample}}$$

Results

Global Proteomics Characterization of Eye and Liver S9 Samples

The data analysis of the complete proteome FASTA file revealed that 269 proteins were specific to the eye sample (Supplemental Table 1),

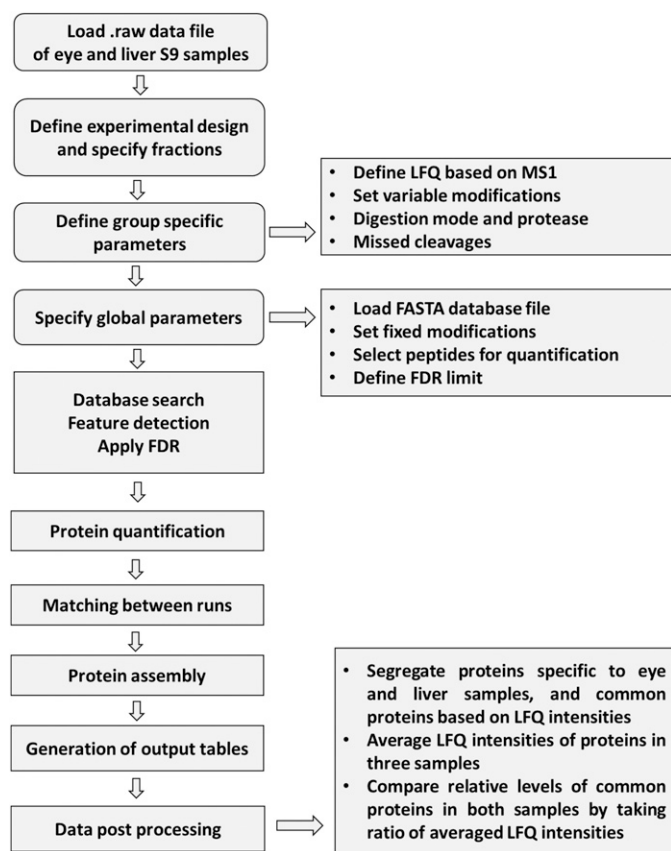


Fig. 1. Workflow employed for the analysis of DDA data of the eye and the liver samples by Maxquant (Tyanova et al., 2016; Beer et al., 2017).

648 of them were specific to the liver (Supplemental Table 2), and 424 proteins were common in both the samples (Supplemental Table 3). On the other hand, out of the total 1187 proteins present in the curated FASTA file, 291 proteins were identified in both the samples. In this case, 23 proteins were specific to the eye (Supplemental Table 4), 174 were restricted to the liver (Supplemental Table 5), and 94 were common to both the organs (Supplemental Table 6). The corresponding Venn diagrams are shown in Fig. 2, A1 and A2, respectively. The significant differences in the total proteins and the metabolizing enzymes are highlighted by the first component of PCA score plots in Fig. 2, B1 and B2, respectively. The string analysis highlighted that most important biologic pathways associated with metabolic proteins identified in the eye were related to cellular response to aldehydes and their detoxification (Supplemental Fig. 1B). It is justified based on our finding of most prominent metabolizing proteins in the eye being the aldehyde dehydrogenases (ALDH), which includes ALDH1A1, ALDH1A3, ALDH4A1, ALDH6A1, ALDH7A1, ALDH9A1, and ALDH3B1. These enzymes tend to be responsible for the metabolism of aldehydic moieties generated during lipid peroxidation, hypoxia, or any other conditions.

The list of proteins identified using the curated FASTA file for the metabolic enzymes was further refined to segregate DMEs. In that respect, only 5 DMEs, which were, RDH5, GSTM2, NQO1, AKR1B1, and ALDH3B1, were found to be specific to the eye S9 fraction. There were 86 DMEs specific to the liver S9 fraction, whereas 24 proteins were common between both the eye and the liver S9 fractions. The final list is provided in Table 1.

Relative Abundance of Proteins in Eye and Liver S9 Fractions

A few proteins among the common ones in the eye and the liver samples showed significant differences in their levels, as highlighted in the volcano plots in Fig. 2C and in Supplemental Tables 3 and 6. Furthermore, the LFQ intensities of 94 common proteins that were detected during proteome screening using the curated FASTA file in the human eye and liver S9 fractions are provided in Fig. 3. Among these proteins, 18 proteins were observed to be predominant in the eye than in the liver (Fig. 4A). In contrast, 43 proteins were predominant in the liver as compared with the eye (Fig. 4B), whereas 33 were comparable in both the samples (Supplemental Table 6). The cut off for the predominance in eye was >2 for the ratio of protein intensities in the eye versus the liver, whereas the same for the liver was <0.5 . The proteins having value within 0.5 to 2 were considered comparable in both the fractions. Of the 24 common DMEs in the eye and the liver S9 fractions, 3 were predominant in the eye, 18 were predominant in the liver, and 3 were comparable between both (Table 2).

Proteins Predominant in Eye as Compared with Liver. The ratio of average LFQ intensities in the eye and the liver samples for 18 predominant proteins in the eye ranged from 2.284 to 150.397 (Fig. 4A; Supplemental Table 6). Among them, GSTP1, H3C1, ATP1A1, APOA1, and THRB showed more than 10 times higher values in the eye as compared with the liver (Fig. 4A; Supplemental Table 6). Interestingly, human prothrombin (THRB) showed ~ 150 times higher relative abundance in the eye.

Three DMEs, in other words, CAH1, GSTM3, and GSTP1, which were predominant in the eye, had more than 4 times higher values of LFQ intensities in the eye as compared with the liver (Table 2).

Proteins Predominant in Liver than Eye. The ratios of intensities in the eye versus the liver samples of 43 proteins, which were predominant in the liver, ranged from 0.002 to 0.491 (Fig. 4B; Supplemental Table 6). Among them, CES1P1, ALDH4A1, and ADH1B showed more than 100 times lower relative abundance in the eye as compared with the liver. There were 14 proteins that showed more than 10 times, whereas 14 proteins showed from 1 to 10 times lower relative abundance in the eye as compared with the liver.

The ratios of intensities for 18 DME proteins ranged from 0.002 to 0.491. The relative abundance of CES1P1, ALDH4A1, and ADH1B were substantially higher in the liver as compared with the eye, whereas CBR1, QOR, ALDH1A1, SELENBP1, ADH5, HSD17B12, and ESD were moderately higher in the liver (Table 2).

Proteins Comparable between Eye and Liver. There were 33 proteins observed to be comparable between both the eye and the liver S9 fractions. The ratio of LFQ intensities ranged from 0.505 to 1.895 (Supplemental Table 6). Among them, 19 proteins had higher values in the liver, whereas 14 proteins had higher values in the eye S9 fraction.

The LFQ intensities of three DMEs, which were ALDH9A1, COX41, and CAH2 were comparable between the eye and the liver samples (Table 2).

Discussion

The main aim of this study was to compare the quantitative proteome of the human eye and the liver with specific emphasis on the abundance of enzymes involved in the metabolism of xenobiotics and endobiotics. We used the lens-free whole eye homogenate to explore its global proteomics profile. The S9 fractions of the eye and the liver allowed direct comparison of the two organs. Although the major DMEs, such as cytochrome P450s, UGTs, and SULTs were not detected in the eye S9 fraction, the isoforms of alcohol dehydrogenases (ADHs), ALDHs, carbonic anhydrases (CAHs), AKRs, esterases, epoxide hydrolases (EPHXs), and GSTs were abundantly detected in the eye (Table 1).

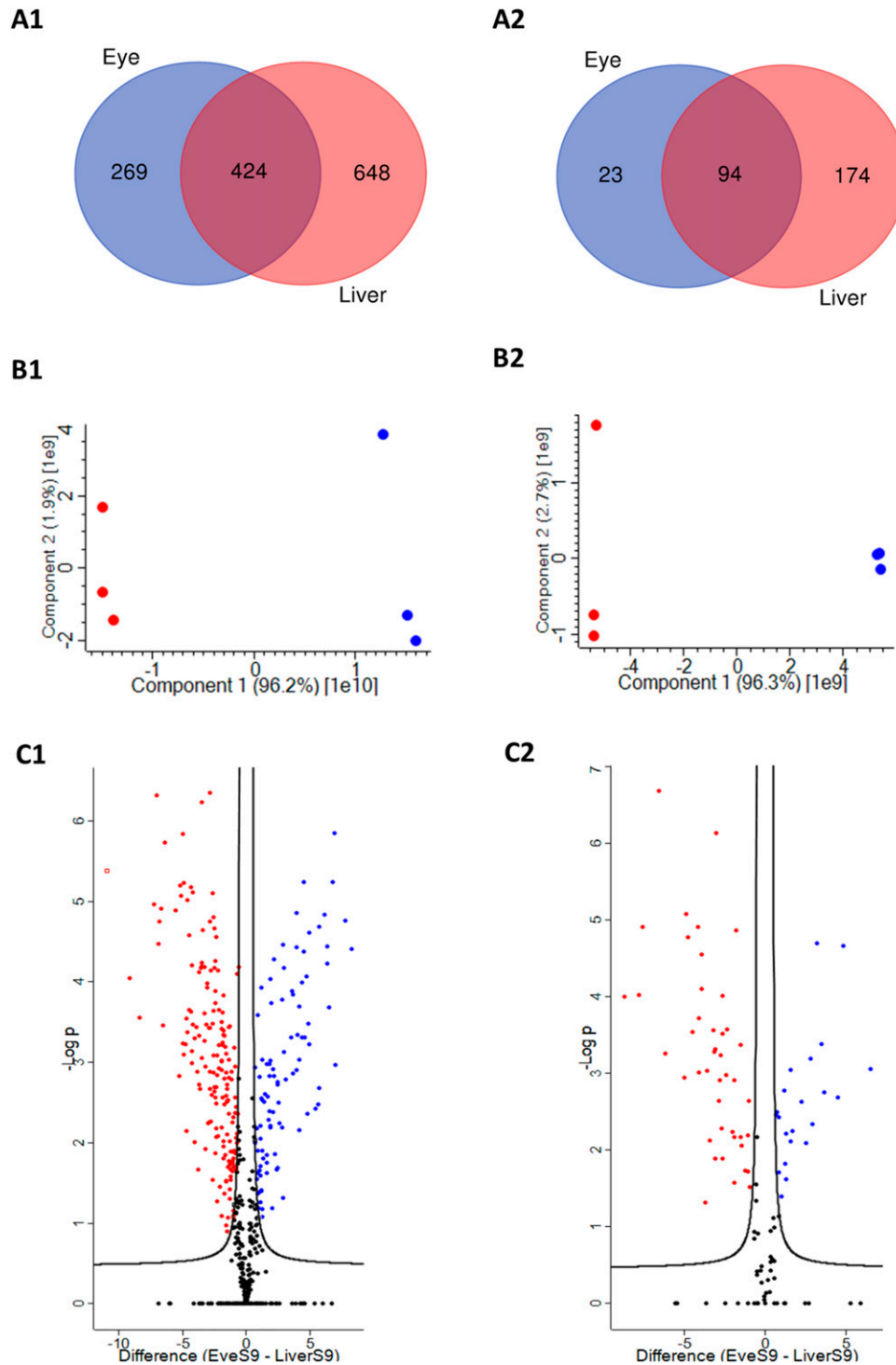


Fig. 2. Differential protein expression of the eye and the liver S9 fractions. (A1) Venn diagram of the total proteins identified in the S9 fractions of eye and liver. (A2) Venn diagram of the total metabolic enzymes identified in the S9 fractions of eye and liver. (B1) PCA score plot between eye and liver proteomes. (B2) PCA score plot between eye and liver metabolic enzymes. The differential clustering of the pooled replicate in PCA plots indicates the significant differences in the proteomic data. (C1) Volcano plot of eye versus liver proteomes. (C2) Volcano plot of eye versus liver metabolic enzymes. In the volcano plots, the x-axis is the fold-change of eye to liver proteomes and y-axis shows $\log P$ value, t test. The black lines in the volcano plots indicate the threshold for the statistical significance with a false discovery rate of 5% and a S_0 of 0.5.

These data are novel hypothesis-generating observations for the future targeted studies.

The presence of ADHs and ALDHs in the eye of preclinical species has been previously reported (Jedziniak and Rokita, 1983; Holmes and

Vandeberg, 1986; Holmes et al., 1988, 1989; Gondhowiardjo et al., 1991; Godbout, 1992). These enzymes have been established to be vital for metabolism of retinoids, especially the conversion of vitamin A (retinol) to retinoic acid. Retinol is oxidized to retinal by ADHs (e.g.,

TABLE 1
List of DMEs identified in eye and liver S9

<i>DMEs specific to eye S9 (05 proteins)</i>
RDH5, GSTM2, NQO1, AKR1B1, and ALDH3B1
<i>DMEs specific to liver S9 (86 proteins)</i>
AADAC, ACOX1, ACOX2, ADH1A, ADH1C, ADH4, ADH6, AKR1B10, AKR1C1, AKR1C2, AKR1C3, AKR1C4, AKR1D1, ALDH1B1, ALDH1L1, ALDH3A2, ALDH8A1, AOX1, BPHL, CES2, COX1, COX2, COX5B, CYP1A2, CYP2A7, CYP2B6, CYP2C8, CYP2C9, CYP2D7, CYP2E1, CYP3A4, CYP3A5, CYP4A11, CYP4F11, CYP4F2, CYP51A1, CYP8B1, DCXR, DECR1, DHRS1, DHRS4L2, DHRS7, EPHX2, FMO4, FMO5, GABT, GSTA5, GSTK1, GSTM1, GSTM4, GSTT1, GSTZ1, HSD11B1, HSD17B11, HSD17B13, HSD17B2, HSD17B4, HSD17B6, HSD17B8, MAOA, MAOB, MAOX, MGST1, MGST3, PON1, PON2, PON3, POR, PTGR1, RDH11, RDH16, SQOR, SULT1A1, SULT2A1, SUOX, UGT1A1, UGT1A10, UGT1A3, UGT1A4, UGT1A7, UGT2A3, UGT2B10, UGT2B15, UGT2B4, UGT2B7, and XDH
<i>DMEs common to eye and liver S9 (24 proteins)</i>
CAH1, GSTM3, GSTP1, CES1P1, ALDH4A1, ADH1B, CYB5A, EPHX1, ALDH7A1, COMT, AKR1A1, ALDH1A3, HSD17B10, GSTO1, CBR1, QOR, ALDH1A1, SELENBP1, ADH5, HSD17B12, ESD, ALDH9A1, COX41, and CAH2

AADAC, arylacetamide deacetylase; ACOX, acyl-coenzyme A oxidase; AOX, aldehyde oxidase; BPHL, biphenyl hydrolase-like protein; DCXR, dicarbonyl/L-xylulose reductase; DECR, 2,4-dienoyl-CoA reductase; DHRS, dehydrogenase/reductase SDR family; ESD, Esterase D (S-formylglutathione hydrolase); FMO, flavin-containing monooxygenase; HSD11B, 11-β-hydroxysteroid; HSD17B, 17-β-hydroxysteroid; MGST, microsomal glutathione S-transferase; MAO, monoamine oxidase; PON, paraoxonase; POR, P450 reductase; PTGR1, prostaglandin reductase 1; SQOR, sulfide:quinone oxidoreductase; XDH, xanthine dehydrogenase.

ADH1B2, ADH4, and RDH5), which subsequently leads to the formation of retinoic acid by the action of ALDHs (e.g., ALDH1A1, ALDH1A2 and ALDH1A3) (Duester 2001; Martras et al., 2004; Gallego et al., 2006; Xiao et al., 2009). Retinoic acid is a critical regulator in a number of cell growth and differentiation pathways, such as spinal cord and retina development during embryogenesis, neuronal cell differentiation, and maintenance of epithelial cell type in adult tissues (Moretti et

al., 2016). Additionally, some ALDHs (e.g., ALDH1A1, ALDH3A1, and ALDH7A1) are also involved in ocular detoxification of aldehydes produced by lipid peroxidation. For example, one of the most toxic and abundant lipid-derivative aldehydes, 4-hydroxynonenal, is detoxified by these enzymes by its oxidation to 4-hydroxy-2-nonenol (Choudhary et al., 2003; Pappa et al., 2003; Xiao et al., 2009; Brocker et al., 2010). The metabolism of levobunolol to dihydrolevobunolol in the

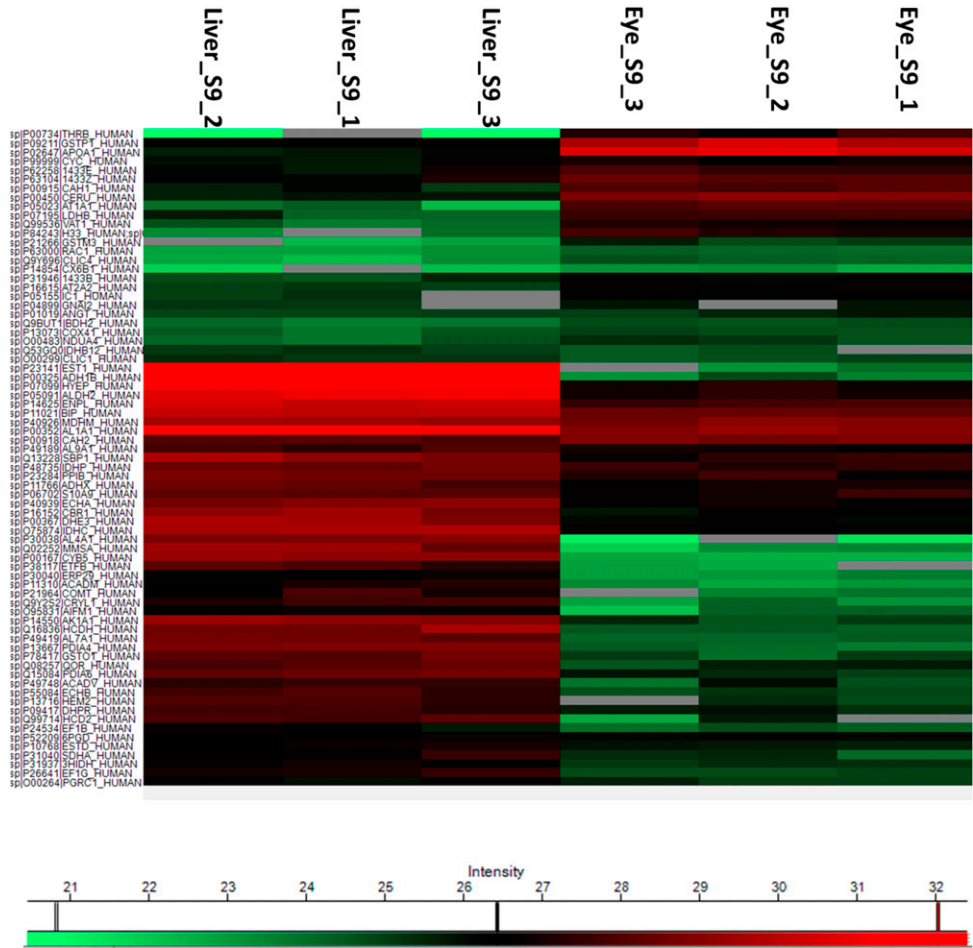


Fig. 3. Heat map representing significantly (p<0.05) different metabolic enzymes between eye and liver S9 fractions. Data were normalized and log transformed.

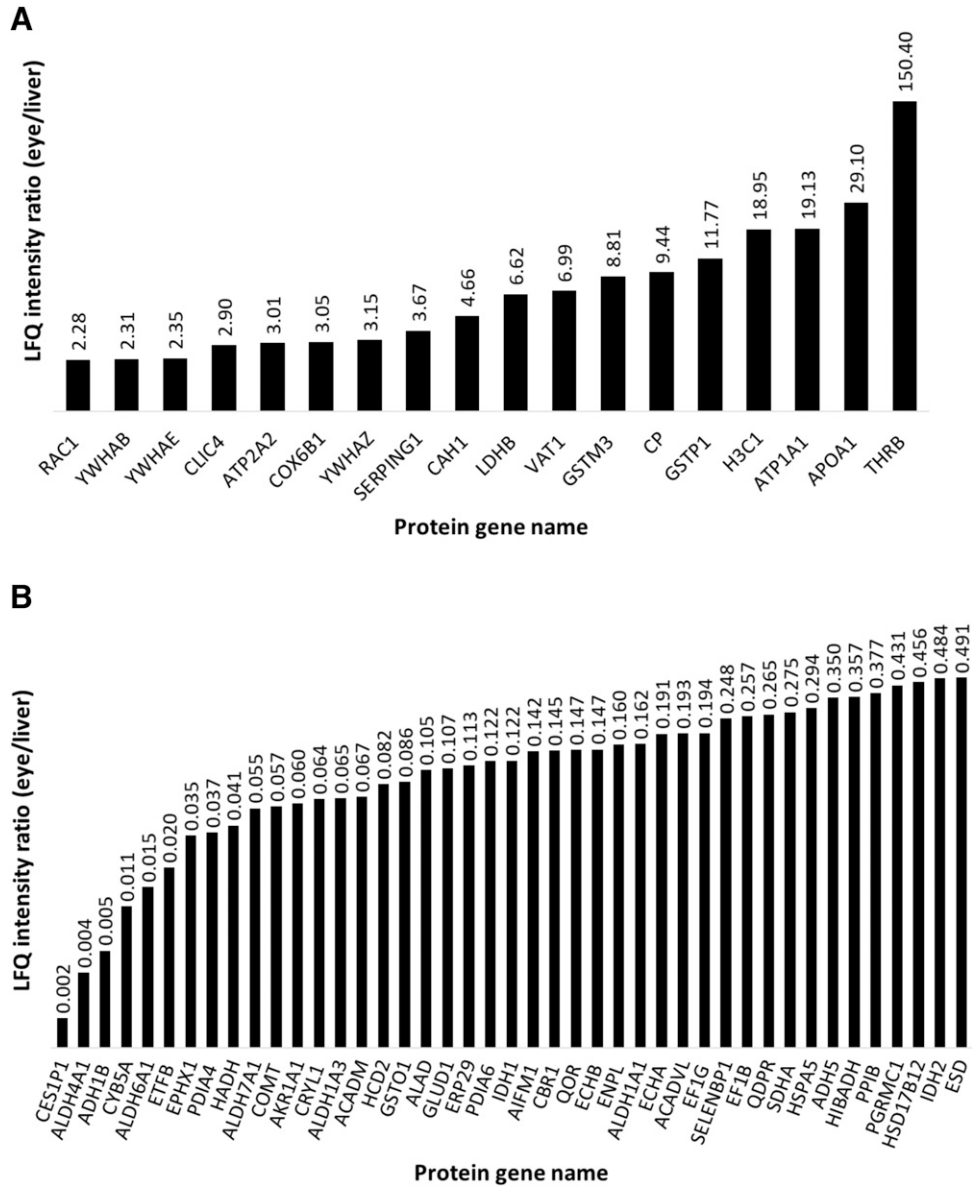


Fig. 4. Relative abundance of DMEs in eye S9 versus liver S9. (A) DMEs predominant in eye S9 than in liver S9 and (B) DMEs predominant in liver S9 than in eye S9. The y-axis is log transformed, and the values of the relative abundance are shown with each bar.

ocular S9 fraction obtained from rat, rabbit, and human eye revealed the presence of AKRs in the eye (Lee et al., 1988). Indeed, dihydrolevobunolol formation is considered as a marker of AKR activity in the eye (Argikar et al., 2016). The presence of carbonyl reductases, AKR1C1,

and AKR1C3 has been postulated in the human eye previously (Dumouchel et al., 2018). These proteins, along with AKR1A1 and AKR1B1 (specific to eye), were also detected in the present study. We also detected zeta crystallin protein or NADPH:quinone oxidoreductase

TABLE 2
Relative levels of common DMEs in eye versus liver*

A. DMEs predominant in eye S9 (03 proteins; eye/liver ratio of LFQ intensities >2)
CAH1 (4.66), GSTM3 (8.81), GSTP1 (11.77)
B. DMEs predominant in liver S9 (18 proteins; eye/liver ratio of LFQ intensities <0.5)
CES1 (0.002), ALDH4A1 (0.004), ADH1B (0.005), CYB5A (0.011), EPHX1 (0.035), ALDH7A1 (0.055), COMT (0.057), AKR1A1 (0.060), ALDH1A3 (0.065), HSD17B10 (0.082), GSTO1 (0.086), CBR1 (0.145), QOR (0.147), ALDH1A1 (0.162), SELENBP1 (0.248), ADH5 (0.350), HSD17B12 (0.456), ESD (0.491)
C. DMEs comparable between eye and liver S9 (03 Proteins; eye/liver ratio of LFQ intensities between 0.5 to 2)
ALDH9A1 (0.524), COX41 (1.41), CAH2 (1.69)

*The ratio of average of LFQ intensities in eye versus liver S9 fractions is given within the brackets.

1 (NOQ1) in the eye S9, which was previously identified in human eyes using immunohistochemical techniques (Schelonka et al., 2000). The evidence for the presence of esterase enzymes in ocular tissues of animals exists in the literature (Lee et al., 1982a, b; Lee, 1983), which have been indicated to be involved in the ocular metabolism of pro-drugs, such as valacyclovir, valganciclovir, and dipivefrin (Wei et al., 1978; Macha and Mitra, 2002; Katragadda et al., 2006). This is consistent with carboxylesterase 4 (CES1P1) detected in the human eye S9 fraction in this study. Similarly, inhibition of epoxide hydrolases has been suggested as a treatment strategy for various ocular diseases, such as diabetic retinopathy, diabetic keratopathy, and age-related macular degeneration (Park et al., 2018; Hu et al., 2019; Park and Corson, 2019). The presence of epoxide hydrolase 1 (EPHX1) in the ocular S9 fraction detected in this study provides a pathway for targeted research to develop new drugs for the eye. The detection of CAH1 and CAH2 in our study in the pooled eye S9 fraction is also consistent with the literature (Lee, 1983; Wistrand et al., 1986). Indeed, these ocular enzymes are targeted for antiglaucoma activity, i.e., acetazolamide (Breinin and Görtz, 1954), dorzolamide (Lippa et al., 1992), and brinzolamide (Silver, 1998).

GST was another major enzyme category that was detected in the eye in our study. Specifically, GSTM2 was observed in the eye, whereas GSTO1, GSTP1, and GSTM3 were common to the eye and the liver. The GST enzyme activity using 1-Chloro-2,4-dinitrobenzene (CDNB), ethacrynic acid, and sulfobromophthalein as probe substrates is also reported elsewhere (Watkins et al., 1991). Even the detection of GST activity or expression is known (Awasthi et al., 1980; Ahmad et al., 1988; Srivastava et al., 1994; Ketterer 1998; Singhal et al., 1999; Yang et al., 2002), and the novelty of present study is that it presents the first accurate and quantitative evidence of specific GST isoforms in the human eye in relation to the liver. Our finding regarding the presence of catechol *O*-methyltransferase (COMT) in the eye is consistent with the enzyme activity in retina-choroid, iris-ciliary body, and optic nerve segments of albino rabbits (Waltman and Sears, 1964). In addition, our results show the presence of eye-specific and eye-predominant DMEs and validate the previously published metabolic reactions for levobunolol (Argikar et al., 2016). Thus, this study provides a comprehensive picture of ocular metabolic functionality.

Although the activity of some cytochrome P450s, UGTs, SULTs, and NATs have been reported in various ocular tissues (Waxman et al., 1988; Watkins et al., 1991; Zhao and Shichi, 1995; Mcavoy et al., 1996; Stoilov et al., 1997; Stoilov et al., 1998; Mastuyugin et al., 1999; Xie et al., 2000; Tsao et al., 2001; Ikeda et al., 2003; Attar et al., 2005b; Zhang et al., 2008; Kölln and Reichl, 2012; Bushee et al., 2015; Argikar et al., 2016; Dumouchel et al., 2017), these proteins were not detected in eye S9 fraction in our study. The potential reasons for the variability are: 1) the source of eye in reported studies was mostly animal; 2) none of the reported studies used a lens-free eye homogenate; 3) the expression of some of these enzymes (e.g., NAT) (Bushee et al., 2015; Dumouchel et al., 2017) were detected in the lens although this study only included the lens-free eye milieu, and 4) below the limits of detection levels of these proteins in our assay in the eye S9 fraction.

The eye has a complex anatomy and physiology, with numerous different cell types and tissues with their individual metabolic capabilities. Studies in individual eye components help in exploring the component-specific (retinal, choroidal, conjunctival etc.) efficacy, metabolism, and toxicity. However, the preparation of in vitro models based on individual eye components require extensive skills in tissue dissection. As pooling of eye components is generally not feasible, most of these studies are limited to single donors. These studies are more confirmatory than exploratory, so their utility is limited when we have little knowledge

about the disposition characteristics of drug. On the other hand, whole eye S9 fraction is an economical and commonly used in vitro alternate for metabolic screening in early discovery to identify soft spots, screen triage compounds, and to drive structure-metabolism relationships during lead optimization. It contains enzymes expressed in both cytosol and endoplasmic reticulum, and can be customized with the cofactors to study specific ocular metabolism questions. However, S9 fractions do not include mitochondrial drug metabolizing enzymes and thus cannot be used to study mitochondrial β -oxidation. Further, S9 fraction is a static model, as it does not account for transport of drugs across the ocular membranes (Dumouchel et al., 2018). We used the lens-free whole eye for S9 preparation, which can't be used to study the role of lens in xenobiotic metabolism. The latter is a limitation because the eye lens is known to possess glutathione *S*-transferase and *N*-acetyltransferase activities (Argikar et al., 2017a). Thus, the information provided in this manuscript is anticipated to be helpful in the physiologically based pharmacokinetic modeling of drugs or endobiotics within the eye, cleared by the proteins identified herein. The developed models will be particularly useful in understanding ocular pharmacokinetics and toxicological behavior of ophthalmic drugs and endobiotics. Based on the comparative eye versus liver proteomics data presented here, and the differences in the sizes of the two organs, ocular metabolism likely plays an insignificant role in drug clearance. However, ocular metabolism can be important in regulating the local efficacy and toxicity of the drugs.

As discussed earlier, one pooled sample was analyzed for both the eye ($n = 11$ donors) as well as the liver ($n = 50$ donors) S9 fractions, which is generally done in studies with tissue banks. The pooled samples only provide the mean estimates of differential tissue abundance without interindividual variability data. Pooling of S9 samples, for this study, was considered 'fit for the purpose' to generate and compare data on ocular versus hepatic metabolism proteome of an average virtual human. Although it is always better to have large sample size for statistical validation of the observed differences, the ocular S9 fractions had limited sample size, the reason being the limitation of time and resource investment and challenges in procurement of enough human eyes. Although the relative proteomics data presented here do not provide a clear picture of the dynamic expression of DMEs in both eye and liver, this report is the foundation on which targeted quantification of eye proteins can be performed to build a comprehensive knowledge bank. Importantly, the comparative proteomics data can be used to scale the absolute levels of DMEs in the eye S9 fractions from the reported liver S9 data.

In summary, the present study entails global proteome profiling of the eye and the liver S9 fractions. The enzymes present in both the samples were identified and quantitatively compared. This study bears great significance in gaining deeper insights of metabolic and bioactivation potential of both systemically as well as topically administered ophthalmic drugs, as well as in endobiotic metabolism within the eye. This investigation provides foundation for subsequent targeted proteomic, genomic, and functional studies to explore the effects of sex, age, genotype, and disease conditions across the populations.

Authorship Contributions

Participated in research design: Balhara, Basit, Argikar, Dumouchel, Singh, Prasad.

Conducted experiments: Basit, Prasad.

Contributed new reagents or analytic tools: Argikar, Dumouchel.

Performed data analysis: Balhara, Basit, Prasad.

Wrote or contributed to the writing of the manuscript: Balhara, Basit, Argikar, Dumouchel, Singh, Prasad.

References

- Ahmad H, Singh SV, Medh RD, Ansari GA, Kurosky A, and Awasthi YC (1988) Differential expression of alpha, mu and pi classes of isozymes of glutathione S-transferase in bovine lens, cornea, and retina. *Arch Biochem Biophys* **266**:416–426.
- Al-Ghananeem AM and Crooks PA (2007) Phase I and phase II ocular metabolic activities and the role of metabolism in ophthalmic prodrug and codrug design and delivery. *Molecules* **12**:373–388.
- Argikar UA, Dumouchel JL, Dunne CE, and Bushee AJ (2017a) Ocular non-P450 oxidative, reductive, hydrolytic, and conjugative drug metabolizing enzymes. *Drug Metab Rev* **49**:372–394.
- Argikar UA, Dumouchel JL, Dunne CE, Saran C, Cirello AL, and Gunduz M (2016) Ocular metabolism of levobunolol: historic and emerging metabolic pathways. *Drug Metab Dispos* **44**:1304–1312.
- Argikar UA, Dumouchel JL, Kramlinger VM, Cirello AL, Gunduz M, Dunne CE, and Sohal B (2017b) Do we need to study metabolism and distribution in the eye: why, when, and are we there yet? *J Pharm Sci* **106**:2276–2281.
- Argikar UA and Remmel RP (2009a) Variation in glucuronidation of lamotrigine in human liver microsomes. *Xenobiotica* **39**:355–363.
- Argikar UA and Remmel RP (2009b) Effect of aging on glucuronidation of valproic acid in human liver microsomes and the role of UDP-glucuronosyltransferase UGT1A4, UGT1A8, and UGT1A10. *Drug Metab Dispos* **37**:229–236.
- Attar M, Ling KHJ, Tang-Liu DD, Neamati N, and Lee VH (2005b) Cytochrome P450 3A expression and activity in the rabbit lacrimal gland: glucocorticoid modulation and the impact on androgen metabolism. *Invest Ophthalmol Vis Sci* **46**:4697–4706.
- Awasthi YC, Saneto RP, and Srivastava SK (1980) Purification and properties of bovine lens glutathione S-transferase. *Exp Eye Res* **30**:29–39.
- Basit A, Neradugomma NK, Wolford C, Fan PW, Murray B, Takahashi RH, Khojasteh SC, Smith BJ, Heyward S, Totah RA, and Kelly EJ (2020). Characterization of differential tissue abundance of major non-CYP enzymes in human. *Mol Pharm* **17**: 4114–4124.
- Beer LA, Liu P, Ky B, Barnhart KT, and Speicher DW (2017) Efficient quantitative comparisons of plasma proteomes using label-free analysis with MaxQuant. *Methods Mol Biol* **1619**:339–352.
- Bhatt DK, Mehrotra A, Gaedigk A, Chapa R, Basit A, Zhang H, Choudhary P, Boberg M, Pearce RE, Gaedigk R, et al. (2019) Age- and genotype-dependent variability in the protein abundance and activity of six major uridine diphosphate-glucuronosyltransferases in human liver. *Clin Pharmacol Ther* **105**:131–141.
- Boberg M, Vrana M, Mehrotra A, Pearce RE, Gaedigk A, Bhatt DK, Leeder JS, and Prasad B (2017) Age-dependent absolute abundance of hepatic carboxylesterases (CES1 and CES2) by LC-MS/MS proteomics: application to PBPK modeling of oseltamivir in vivo pharmacokinetics in infants. *Drug Metab Dispos* **45**:216–223.PubMed
- Breinin GM and Götz H (1954) Carbonic anhydrase inhibitor acetazolamide (diamox); a new approach to the therapy of glaucoma. *AMA Arch Ophthalmol* **52**:333–348.
- Brocker C, Lassen N, Estey T, Pappa A, Cantore M, Orlova VV, Chavakis T, Kavanagh KL, Oppermann U, and Vasilou V (2010). Aldehyde dehydrogenase 7A1 (ALDH7A1) is a novel enzyme involved in cellular defense against hyperosmotic stress. *J Biol Chem* **285**:18452–63.
- Bushee JL, Dunne CE, and Argikar UA (2015) An in vitro approach to investigate ocular metabolism of a topical, selective β_1 -adrenergic blocking agent, betaxolol. *Xenobiotica* **45**:396–405.
- Choudhary S, Srivastava S, Xiao T, Andley UP, Srivastava SK, and Ansari NH (2003) Metabolism of lipid derived aldehyde, 4-hydroxynonenal in human lens epithelial cells and rat lens. *Invest Ophthalmol Vis Sci* **44**:2675–2682.
- Cirello AL, Dumouchel JL, Gunduz M, Dunne CE, and Argikar UA (2017) In vitro ocular metabolism and bioactivation of ketoconazole in rat, rabbit and human. *Drug Metab Pharmacokinet* **32**:121–126.
- Connors MS, Stoltz RA, Davis KL, Dunn MW, Abraham NG, Levere RD, and Laniado-Schwartzman M (1995) A closed eye contact lens model of corneal inflammation. Part 2: Inhibition of cytochrome P450 arachidonic acid metabolism alleviates inflammatory sequelae. *Invest Ophthalmol Vis Sci* **36**:841–850.
- Couto N, Al-Majdoub ZM, Achour B, Wright PC, Rostami-Hodjegan A, and Barber J (2019) Quantification of proteins involved in drug metabolism and disposition in the human liver using label-free global proteomics. *Mol Pharm* **16**:632–647.
- Couto N, Al-Majdoub ZM, Gibson S, Davies PJ, Achour B, Harwood MD, Carlson G, Barber J, Rostami-Hodjegan A, and Warhurst G (2020) Quantitative proteomics of clinically relevant drug-metabolizing enzymes and drug transporters and their intercorrelations in the human small intestine. *Drug Metab Dispos* **48**:245–254.
- Cox J, Hein MY, Luber CA, Paron I, Nagaraj N, and Mann M (2014) Accurate proteome-wide label-free quantification by delayed normalization and maximal peptide ratio extraction, termed MaxLFQ. *Mol Cell Proteomics* **13**:2513–2526.
- Drozdzik M, Busch D, Lapczuk J, Müller J, Ostrowski M, Kurzawski M, and Oswald S (2018) Protein abundance of clinically relevant drug-metabolizing enzymes in the human liver and intestine: a comparative analysis in paired tissue specimens. *Clin Pharmacol Ther* **104**:515–524.
- Duester G (2001) Genetic dissection of retinoid dehydrogenases. *Chem Biol Interact* **130**:132–469–480.
- Dumouchel JL, Argikar UA, Spear J, Brown A, Dunne CE, Kramlinger VM, Cirello AL, and Gunduz M (2017) Investigation of ocular bioactivation potential and the role of cytochrome P450 2D enzymes in rat. *Drug Metab Lett* **11**:102–110.
- Dumouchel JL, Chemuturi N, Milton MN, Camenisch G, Chastain J, Walles M, Sasseville V, Gunduz M, Iyer GR, and Argikar UA (2018) Models and approaches describing the metabolism, transport, and toxicity of drugs administered by the ocular route. *Drug Metab Dispos* **46**:1670–1683.
- Gallego O, Belyaeva OV, Porté S, Ruiz FX, Stetsenko AV, Shabrova EV, Kostereva NV, Farrés J, Parés X, and Kedishvili NY (2006) Comparative functional analysis of human medium-chain dehydrogenases, short-chain dehydrogenases/reductases and aldo-keto reductases with retinoids. *Biochem J* **399**:101–109.
- Garcia GA, Ngai P, Mosaed S, and Lin KY (2016) Critical evaluation of latanoprostene banded in the treatment of glaucoma. *Clin Ophthalmol* **10**:2035–2050.
- Godbout R (1992) High levels of aldehyde dehydrogenase transcripts in the undifferentiated chick retina. *Exp Eye Res* **54**:297–305.
- Gokulgandhi MR, Vadlapudi AD, and Mitra AK (2012) Ocular toxicity from systemically administered xenobiotics. *Expert Opin Drug Metab Toxicol* **8**:1277–1291.
- Gondhwardijo TD, van Haeringen NJ, Hoekzema R, Pels L, and Kijlstra A (1991) Detection of aldehyde dehydrogenase activity in human corneal extracts. *Curr Eye Res* **10**:1001–1007.
- Holmes RS and Vandeberg JL (1986) Ocular NAD-dependent alcohol dehydrogenase and aldehyde dehydrogenase in the baboon. *Exp Eye Res* **43**:383–396.
- Holmes RS, Cheung B, and VandeBerg JL (1989) Isoelectric focusing studies of aldehyde dehydrogenases, alcohol dehydrogenases and oxidases from mammalian anterior eye tissues. *Comp Biochem Physiol B* **93**:271–277.
- Holmes RS, Popp RA, and VandeBerg JL (1988) Genetics of ocular NAD⁺-dependent alcohol dehydrogenase and aldehyde dehydrogenase in the mouse: evidence for genetic identity with stomach isozymes and localization of Ahd-4 on chromosome 11 near trembler. *Biochem Genet* **26**:191–205.
- Hu J, Bibli SI, Wittig J, Zukunft S, Lin J, Hammes HP, Popp R, and Fleming I (2019) Soluble epoxide hydrolase promotes astrocyte survival in retinopathy of prematurity. *J Clin Invest* **129**:5204–5218.
- Ikeda H, Ueda M, Ikeda M, Kobayashi H, and Honda Y (2003) Oxysterol 7alpha-hydroxylase (CYP39A1) in the ciliary nonpigmented epithelium of bovine eye. *Lab Invest* **83**:349–355.
- Jedziniak J and Rokita J (1983) Aldehyde metabolism in the human lens. *Exp Eye Res* **37**:119–127.
- Kam RKT, Deng Y, Chen Y, and Zhao H (2012) Retinoic acid synthesis and functions in early embryonic development. *Cell Biosci* **2**:11–25.PubMed
- Katragadda S, Talluri RS, and Mitra AK (2006) Simultaneous modulation of transport and metabolism of acyclovir prodrugs across rabbit cornea: an approach involving enzyme inhibitors. *Int J Pharm* **320**:104–113.
- Ketterer B (1998) Glutathione S-transferases and prevention of cellular free radical damage. *Free Radic Res* **28**:647–658.PubMed
- Kölln C and Reichl S (2012) mRNA expression of metabolic enzymes in human cornea, corneal cell lines, and hemi-cornea constructs. *J Ocul Pharmacol Ther* **28**:271–277.
- Kumar D, Yadav AK, and Dash D (2017) Choosing an optimal database for protein identification from tandem mass spectrometry data. *Methods Mol Biol* **1549**:17–29.
- Lee VH (1983) Esterase activities in adult rabbit eyes. *J Pharm Sci* **72**:239–244.
- Lee VH, Chien DS, and Sasaki H (1988) Ocular ketone reductase distribution and its role in the metabolism of ocularly applied levobunolol in the pigmented rabbit. *J Pharmacol Exp Ther* **246**:871–878.
- Lee VH, Imoto DS, and Takemoto KA (1982a) Subcellular distribution of esterases in the bovine eye. *Curr Eye Res* **2**:69–76.
- Lee VH, Morimoto KW, and Stratford RE (1982b) Esterase distribution in the rabbit cornea and its implications in ocular drug bioavailability. *Biopharm Drug Dispos* **3**:291–300.
- Levin W, Lu AY, Ryan D, West S, Kuntzman R, and Conney AH (1972) Partial purification and properties of cytochromes P-450 and P-448 from rat liver microsomes. *Arch Biochem Biophys* **153**:543–553.
- Lippa EA, Carlson LE, Ehinger B, Eriksson LO, Finnström K, Holmin C, Nilsson SE, Nyman K, Raita C, Ringvold A, et al. (1992) Dose response and duration of action of dorzolamide, a topical carbonic anhydrase inhibitor. *Arch Ophthalmol* **110**:495–499.
- Macha S and Mitra AK (2002) Ocular disposition of ganciclovir and its monoester prodrugs following intravitreal administration using microdialysis. *Drug Metab Dispos* **30**:670–675.
- Mastyugin V, Aversa E, Bonazzi A, Vafaei C, Miéyal P, and Schwartzman ML (1999) Hypoxia-induced production of 12-hydroxyeicosanoids in the corneal epithelium: involvement of a cytochrome P-450B1 isoform. *J Pharmacol Exp Ther* **289**:1611–1619.
- Martras S, Álvarez R, Gallego O, Domínguez M, de Lera AR, Farrés J, and Parés X (2004) Kinetics of human alcohol dehydrogenase with ring-oxidized retinoids: effect of Tween 80. *Arch Biochem Biophys* **430**:210–217.PubMed
- McAvoy M, Singh AK, and Shichi H (1996) In situ hybridization of Cyp1a1, Cyp1a2 and Ah receptor mRNAs expressed in murine ocular tissues. *Exp Eye Res* **62**:449–452.
- Moretti A, Li J, Donini S, Sobol RW, Rizzi M, and Garavaglia S (2016) Crystal structure of human aldehyde dehydrogenase IA3 complexed with NAD⁺ and retinoic acid. *Sci Rep* **6**:35710.
- Nakano M, Lockhart CM, Kelly EJ, and Rettie AE (2014) Ocular cytochrome P450s and transporters: roles in disease and endobiotic and xenobiotic disposition. *Drug Metab Rev* **46**:247–260.
- Nakamura K, Hirayama-Kurogi M, Ito S, Kuno T, Yoneyama T, Obuchi W, Terasaki T, and Ohtsuki S (2016) Large-scale multiplex absolute protein quantification of drug-metabolizing enzymes and transporters in human intestine, liver, and kidney microsomes by SWATH-MS: comparison with MRM/MS and HR-MRM/MS. *Proteomics* **16**:2106–2117.
- Oesch F, Fabian E, and Landsiedel R (2019) Xenobiotic-metabolizing enzymes in the lung of experimental animals, man and in human lung models. *Arch Toxicol* **93**:3419–3489.
- Pappa A, Estey T, Manzer R, Brown D, and Vasilou V (2003) Human aldehyde dehydrogenase 3A1 (ALDH3A1): biochemical characterization and immunohistochemical localization in the cornea. *Biochem J* **376**:615–623.
- Park B and Corson TW (2019) Soluble epoxide hydrolase inhibition for ocular diseases: vision for the future. *Front Pharmacol* **10**:95.
- Park B, Pasha SPBS, Si Y, Meroueh SO, Seo SY, and Corson TW (2018) Characterization of a novel inhibitor of soluble epoxide hydrolase and role in ocular neovascularization. *FASEB J* **32**(Suppl 1):561.
- Resing KA, Meyer-Arendt K, Mendoza AM, Aveline-Wolf LD, Jonscher KR, Pierce KG, Old WM, Cheung HT, Russell S, Wattawa JL, et al. (2004) Improving reproducibility and sensitivity in identifying human proteins by shotgun proteomics. *Anal Chem* **76**:3556–3568.
- Scheltonka LP, Siegel D, Wilson MW, Meininger A, and Ross D (2000) Immunohistochemical localization of NQO1 in epithelial dysplasia and neoplasia and in donor eyes. *Invest Ophthalmol Vis Sci* **41**:1617–1622.
- Silver LH; Brinzolamide Primary Therapy Study Group (1998) Clinical efficacy and safety of brinzolamide (Azopt), a new topical carbonic anhydrase inhibitor for primary open-angle glaucoma and ocular hypertension. *Am J Ophthalmol* **126**:400–408.
- Singhal SS, Godley BF, Chandra A, Pandya U, Jin GF, Saini MK, Awasthi S, and Awasthi YC (1999) Induction of glutathione S-transferase hGST 5.8 is an early response to oxidative stress in RPE cells. *Invest Ophthalmol Vis Sci* **40**:2652–2659.
- Srivastava SK, Singhal SS, Bajpai KK, Chaubey M, Ansari NH, and Awasthi YC (1994) A group of glutathione S-transferase isozymes showing high activity towards 4-hydroxy-2-nonenal are present in bovine ocular tissues. *Exp Eye Res* **59**:151–159.
- Stoilov I, Akarsu AN, Alozie I, Child A, Barsom-Homsky M, Turacli ME, Or M, Lewis RA, Ozdemir N, Brice G, et al. (1998) Sequence analysis and homology modeling suggest that primary congenital glaucoma on 2p21 results from mutations disrupting either the hinge region or the conserved core structures of cytochrome P450B1. *Am J Hum Genet* **62**:573–584.
- Stoilov I, Akarsu AN, and Sarfarazi M (1997) Identification of three different truncating mutations in cytochrome P450B1 (CYP1B1) as the principal cause of primary congenital glaucoma

- (Buphthalmos) in families linked to the GLC3A locus on chromosome 2p21. *Hum Mol Genet* **6**:641–647.
- Stoltz RA, Connors MS, Dunn MW, and Schwartzman ML (1994) Effect of metabolic inhibitors on arachidonic acid metabolism in the corneal epithelium: evidence for cytochrome P450-mediated reactions. *J Ocul Pharmacol* **10**:307–317.
- Thrimawithana TR, Young S, Bunt CR, Green C, and Alany RG (2011) Drug delivery to the posterior segment of the eye. *Drug Discov Today* **16**:270–277.
- Tsao CC, Coulter SJ, Chien A, Luo G, Clayton NP, Maronpot R, Goldstein JA, and Zeldin DC (2001) Identification and localization of five CYP2Cs in murine extrahepatic tissues and their metabolism of arachidonic acid to regio- and stereoselective products. *J Pharmacol Exp Ther* **299**:39–47.
- Tyanova S and Cox J (2018) Perseus: a bioinformatics platform for integrative analysis of proteomics data in cancer research, in *Cancer Systems Biology. Methods in Molecular Biology* (Von Stechow L, ed) pp 133–148, Humana Press, New York.
- Tyanova S, Temu T, and Cox J (2016) The MaxQuant computational platform for mass spectrometry-based shotgun proteomics. *Nat Protoc* **11**:2301–2319.
- Waltman S and Sears M (1964) Catechol-O-methyl transferase and monoamine oxidase activity in the ocular tissues of albino rabbits. *Invest Ophthalmol* **3**:601–605.
- Watkins 3rd JB, Wirthwein DP, and Sanders RA (1991) Comparative study of phase II biotransformation in rabbit ocular tissues. *Drug Metab Dispos* **19**:708–713.
- Waxman DJ, Attisano C, Guengerich FP, and Lapenson DP (1988) Human liver microsomal steroid metabolism: identification of the major microsomal steroid hormone 6 beta-hydroxylase cytochrome P-450 enzyme. *Arch Biochem Biophys* **263**:424–436.
- Wei CP, Anderson JA, and Leopold I (1978) Ocular absorption and metabolism of topically applied epinephrine and a dipivalyl ester of epinephrine. *Invest Ophthalmol Vis Sci* **17**:315–321.
- Wistrand PJ, Schenholm M, and Lönnerholm G (1986) Carbonic anhydrase isoenzymes CA I and CA II in the human eye. *Invest Ophthalmol Vis Sci* **27**:419–428.
- Xiao T, Shueb M, Siddiqui MS, Zhang M, Ramana KV, Srivastava SK, Vasiliou V, and Ansari NH (2009) Molecular cloning and oxidative modification of human lens ALDH1A1: implication in impaired detoxification of lipid aldehydes. *J Toxicol Environ Health A* **72**:577–584.
- Xie Q, Zhang QY, Zhang Y, Su T, Gu J, Kaminsky LS, and Ding X (2000) Induction of mouse CYP2J by pyrazole in the eye, kidney, liver, lung, olfactory mucosa, and small intestine, but not in the heart. *Drug Metab Dispos* **28**:1311–1316.
- Yang Y, Sharma R, Cheng JZ, Saini MK, Ansari NH, Andley UP, Awasthi S, and Awasthi YC (2002) Protection of HLE B-3 cells against hydrogen peroxide- and naphthalene-induced lipid peroxidation and apoptosis by transfection with hGSTA1 and hGSTA2. *Invest Ophthalmol Vis Sci* **43**:434–445.
- Yen CY, Russell S, Mendoza AM, Meyer-Arendt K, Sun S, Cios KJ, Ahn NG, and Resing KA (2006) Improving sensitivity in shotgun proteomics using a peptide-centric database with reduced complexity: protease cleavage and SCX elution rules from data mining of MS/MS spectra. *Anal Chem* **78**:1071–1084.
- Zhang T, Xiang CD, Gale D, Carreiro S, Wu EY, and Zhang EY (2008) Drug transporter and cytochrome P450 mRNA expression in human ocular barriers: implications for ocular drug disposition. *Drug Metab Dispos* **36**:1300–1307.
- Zhao C and Shichi H (1995) Immunocytochemical study of cytochrome P450 (1A1/1A2) induction in murine ocular tissues. *Exp Eye Res* **60**:143–152.

Address correspondence to: Dr. Bhagwat Prasad, Department of Pharmaceutical Sciences, Washington State University, 412 E Spokane Falls Blvd., Spokane, WA. E-mail: bhagwat.prasad@wsu.edu; or Dr. Saranjit Singh, Department of Pharmaceutical Analysis, National Institute of Pharmaceutical Education and Research (NIPER), Sector 67, S.A.S. Nagar, Punjab, India. E-mail: ssingh@niper.ac.in
